

A coincidence technique for the study of intense laser atom interactions

B. Witzel^{1,a}, N.A. Papadogiannis¹, and D. Charalambidis^{1,2}¹ Foundation for Research and Technology - Hellas, Institute of Electronic Structure and Laser, Laser and Applications Division, P.O. Box 1527, 71110 Heraklion, Crete, Greece² Department of Physics, University of Crete, P.O. Box 2208, 71003 Heraklion, Crete, Greece

Received 22 November 1999

Abstract. A new device for charged particle coincidence experiments in strong-field, short pulse laser-atom/molecule interactions is presented. The device consists of a single time of flight spectrometer, common for both positive and negative charge detection. Experimental parameters required for the use of the device in the high intensity regime are discussed. A demonstration of electron-ion coincidence measurements in the interaction of Xe atoms with 60 fs laser pulses at 800 nm and an intensity of 4×10^{13} W/cm² is reported.

PACS. 32.80.Gc Photodetachment of atomic negative ions – 32.80.Rm Multiphoton ionization and excitation to highly excited states (e.g., Rydberg states) – 39.30.+w Spectroscopic techniques

1 Introduction

Short pulse duration high intensity laser radiation interaction with atomic or molecular systems has been a fascinating field of research that has led to the observation of several novel phenomena. Aside from higher order harmonic generation (HOHG) [1], which will not be discussed in the present work, the observations that constitute the source of information for the problems under investigation concern multiple charge state distributions, multiphoton or tunneling, over the barrier ionization, [2] or fragmentation [3] measured through ion mass spectroscopy and the above threshold ionization (ATI) [4] measured through high resolution electron spectroscopy. A series of interesting problems on the topic have been addressed in several laboratories during the last 20 years, such as direct *vs.* sequential multiple ionization [5] perturbative *vs.* non-perturbative behavior of the system [6], origin of “plateaus” [7] in photoelectron spectra and side lobes in photoelectron angular distributions [8], ionic contributions [9], non-vertical dissociation [10] and bond softening [11], to mention some of them. Different frequency regimes and pulse lengths have already been investigated. At the same time several models describing the interaction of an atomic or molecular system with strong, short laser pulses [12] have been proposed most of which are still subject to verification. In most of the above experimental investigations simple ion mass or electron spectroscopy has been employed. Initially these techniques provided sufficient sensitivity for studying the vast majority of these effects. However, as the field matures detailed investigations

through more sophisticated experimental approaches become necessary. One such example is the case of ATI spectra. Although they include electrons originating from double or multiple ionization, which may be as high as 10% of the total ($I = 4 \times 10^{13}$ W/cm²), those electrons have been ignored in the analysis and interpretation of the data. Strong field interactions are associated with high degree of excitation and hence multiple correlated decay channels. Thus correlated measurements are expected to give additional and detailed information towards a better understanding of the observed phenomena and provide a proper test ground for models. Few attempts have been made in this direction in the past and were mainly based in statistical methods such as covariance mapping [3]. Only one other investigation using coincidence measurement was applied to a study of direct double ionization [13]. Very recent attempts using ion-recoil spectroscopy and electron-ion coincidence measurements (including this work) are under development in a few laboratories [14].

In the present work we present a new experimental method for charged particle coincidence measurements, in short pulse, high intensity laser-atom/molecule interactions. The method is applied in an electron-ion coincidence experiment in Xe interacting with 60 fs long Ti:sapphire laser pulses. This work is aimed at demonstrating the feasibility of the method and the extent of its applicability. We discuss the important experimental parameters required for the successful use of such a device in the high intensity regime. The results presented here give evidence that correlated measurements may provide information about the importance and possible weighting of the different contributions to the ionization process, thus facilitating the validation of the existing models.

^a e-mail: witzel@uni-freiburg.de

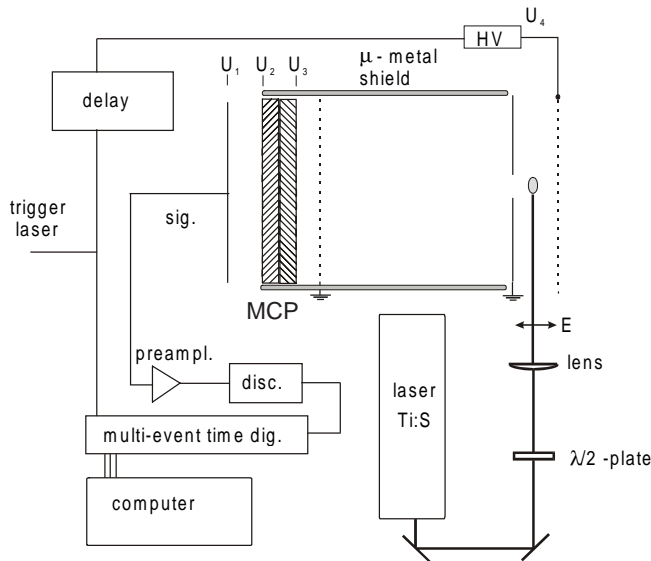


Fig. 1. Experimental set up. Laser source: titanium sapphire with 60 fs pulse duration, 800 nm wavelength and 1 kHz repetition rate. One common electron and ion time of flight tube with delayed pulsed ion extraction voltage and one common electron and ion chevron type MCP detector is used. Recording occurs shot to shot through a multi-event time digitizer. The used voltages are $U_1 = 2500$ V, $U_2 = 2300$ V, $U_3 = 200$ V, $U_4 = 8000$ V.

2 Experimental set up and method

The experimental set-up used is shown in Figure 1. It consists of the laser, the beam delivery subsystem and the subsystem for the charged particle coincidence measurement.

The laser employed is a titanium sapphire oscillator amplified in a regenerative amplifier utilizing a chirped pulse amplification technique [15]. The laser operates at ~ 800 nm and 1 kHz repetition rate, with a measured pulse duration of ~ 60 fs. The maximum energy output of the system is 1 mJ. In the present experiments only 7–12 μ J have been used in order to satisfy the single event condition required in coincidence experiments as discussed below. The beam was focused by a 15 cm focal length lens in to the interaction region, resulting in a maximum intensity of 4×10^{13} W/cm². A half-wave plate is used to control the polarization of the laser.

The charged particle coincidence measurement unit uses one and the same “time of flight” tube and detector for the ionic m/q determination and the electron energy analysis, m and q being the mass and the charge of the ion. The system is located in a vacuum chamber kept at a background pressure lower than 10^{-9} mbar, which is the lowest measurable pressure by the ionization gauges used in this experiment. Pressure considerations in relation to coincidence-measurement requirements will be discussed below. Electrons produced during the interaction of the atoms with the laser radiation drift through a 28 cm field free region towards the chevron type micro-channel plate (MCP) detector. The biasing potentials of the

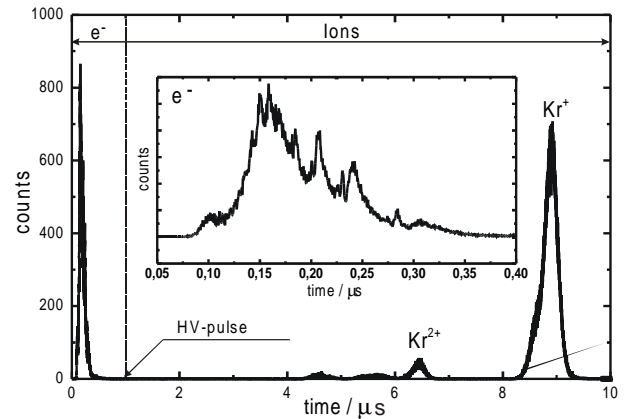


Fig. 2. Total measured spectrum for Kr consisting of 10^6 accumulated traces at a pressure of 10^{-7} mbar. The electron spectrum appears in the first 0.5 μ s of the time of flight spectrum while the ion time of flight spectrum starts at $t = 1$ μ s.

detector U_3 , U_2 and U_1 shown in Figure 1 are 200, 2300 and 2500 V respectively. The angle of acceptance is defined through the effective diameter of the MCP detector to be $< 4^\circ$. An entrance aperture of 5 mm diameter is used in order to reduce the number of the detected background ionization events. The background counts originate from species with lower ionization thresholds than Xe which consequently ionize more efficiently in low intensity regions of the spatial intensity distribution in the vicinity of the focus. It is worth noting that the Brownian motion of the species and the dimensions of the ionizing volume define the minimum dimensions of this aperture that can be used. The polarization of the laser is linear and parallel to the time of flight tube axis. A few mm before the electrons hit the detector they are accelerated through a 200 volt bias in order to achieve maximum detection efficiency at the detector. 1 μ s after the laser atom interaction a 200 ns long voltage pulse of 8000 volts is applied in the interaction region. The pulse accelerates the ionic species, which subsequently fly in the field free region towards the detector. Thus the recorded traces contain both the electron and ion time of flight spectrum. The detector signal passes through a pulse height discriminator and is recorded shot to shot by a multi-event time-digitizer card with a temporal resolution of 0.5 ns, connected to a personal computer (PC). Data are trace by trace transferred and stored in the PC. Under the delayed pulsed voltage used and “time of flight” tube length the electron and ion spectra are well-separated in time. The electron spectrum appears in the first 0.5 μ s of the time of flight spectrum, while the ion time of flight spectrum starts at $t = 1$ μ s. Such a total, combined electron-ion spectrum for Kr is shown in Figure 2. It consists of 10^6 accumulated traces with no coincidence condition set. For this demonstration measurement a relatively high Kr gas pressure of 10^{-7} mbar is used. The ATI peaks are clearly observable in the first part of the spectrum while the different charge states of Kr are resolved at times longer than 6 μ s. Background gas masses are also observable in the spectrum.

Table 1. Number of ions produced per pulse at the focus (150 mm lens) in a volume where the laser intensity drops to the $1/e$ of its maximum value, estimated for different gas pressures assuming a Gaussian spatial distribution and saturation of ionization. Evaluation of the fulfillment of the single event condition

p / mbar	ion / pulse	Fulfillment of the single event condition
10^{-7}	740	no
10^{-8}	74	no
10^{-9}	7	no
10^{-10}	0.7	no
10^{-11}	0.07	yes

The shot by shot acquired and stored traces can then be later analyzed setting the required coincidence condition.

The gas is fed to the vacuum chamber in a continuous flow regulated through a variable leak. For the coincidence measurement the Xe gas pressure was set at $< 3 \times 10^{-9}$ mbar. These pressure conditions and the laser intensities utilized fulfilled single event counting requirements. In order to minimize the number of false coincidences a single event detection requirement has to be satisfied, that is for each laser pulse no more than one ion and one or at most two electrons (double ionization) has to be produced. An acceptable value for the averaged number of produced ions per pulse is $n = 0.2$ to $n = 0.3$ [16]. Assuming a Gaussian spatial distribution the number of ions produced per pulse at the focus (150 mm lens) has been estimated for different gas pressures. In this estimation the volume is taken to be extending up to where the laser intensity drops to the $1/e$ of its maximum value and in this volume ionization is assumed to be saturated. The result is shown in Table 1. One can clearly see that pressures lower than 10^{-10} mbar is required for coincidence measurements in the saturated ionization region. Figure 3 shows measured ion yields of different charge states of Xe as a function of laser intensity. In the same figure the highest intensity for which the single event condition holds is depicted for three different gas pressures. This graph indicates that one has to work below saturation unless the residual gas pressure can be reduced below 10^{-11} mbar.

In order to satisfy the single event condition in the present experiment, the above given pressure and laser intensity values are chosen such as to result in a detection rate of 10 Hz, or equivalently one detected ionization event per 100 laser pulses. Another important parameter for the minimization of false coincidences is the background pressure because ionization of the residual gases occurs much more efficiently than multiple ionization of Xe. A further parameter that has to be considered is the detection efficiency of the detector, which has to be as high as possible. Operating the MCP at 2100 volt, accelerating the electrons with 200 volts and the ions with more than 5 kvolts, the detection efficiency of the MCP detector is estimated to 0.3 for the electrons and 0.4 for the ions [17].

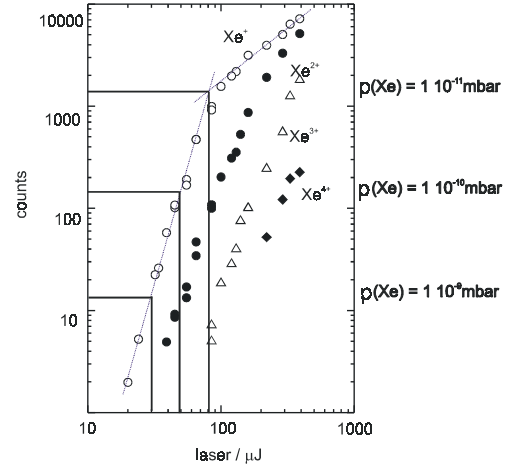


Fig. 3. Measured ion yields of different charge states of Xe. $10 \mu\text{J}$ correspond to $4 \times 10^{13} \text{ W/cm}^2$. The straight lines indicate the intensity limits *vs.* pressure for which the single event condition is satisfied at saturation.

3 Results

Figure 4 shows a typical set of Xe spectra obtained under the conditions given above. Shown in Figure 4a are the total ion (right) and total electron (top) time of flight spectra, as well as the correlated events (middle). In the ionic and correlated spectra only the m/q region between the Xe^+ and Xe^{2+} has been taken into account. Background gas masses appearing outside this region are not shown here. The coincidence condition set for the selection of the correlated events is the appearance of only one electron and one ion per acquisition trace. Thus all the selected traces shown consist of two counts, one corresponding to an electron and one corresponding to a Xe^+ or Xe^{2+} ion. Figure 4b shows the electron energy spectrum and the distribution of the two charge states. The total spectra shown is the average of 1×10^7 traces. The acquisition duration of such a spectrum is 8 hours. This is at the limits of the acquisition duration under stable conditions. Thus for the experimental set up used statistics may be increased only by adding up results of different runs.

At the used laser intensity, the ratio of $\text{Xe}^{2+}/\text{Xe}^+$ yield is approximately $1/9$. The total electron spectrum (electrons from the single and multiple ionization of Xe and background molecules) shows partially resolved ATI peak structure. The low energy part of the spectrum depicts a relatively constant envelope. In the region between 4 and 12 eV the spectrum depicts a rapidly decreasing envelope, while at higher energies the electron yield first remains almost constant and finally drops towards zero at around 25 eV. Thus the well-known ATI characteristics, including the “plateau” in the region between 15 and 22 eV, are present in the spectrum of Figure 4b. From the 1×10^7 traces acquired only 46 fulfill the coincidence condition of observing one electron and one Xe^+ or Xe^{2+} ion. In particular only 6 events correlate with double ionization. This is mainly due to the very low electron detection

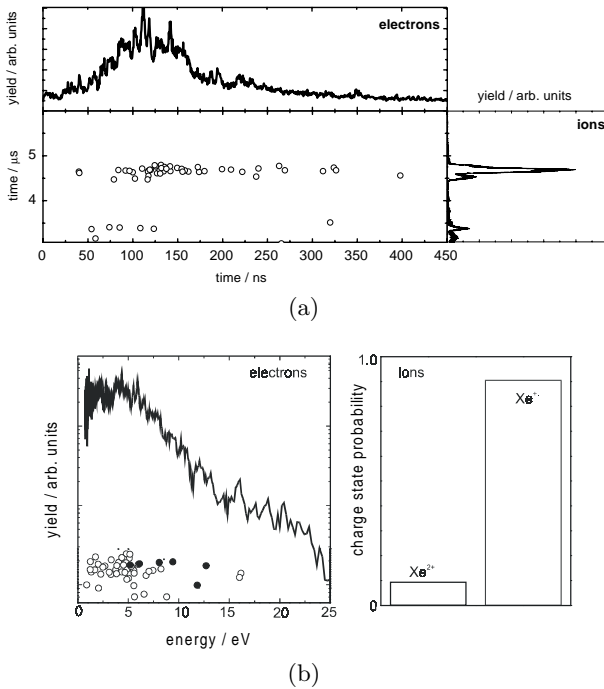


Fig. 4. Typical Xe time of flight spectra obtained under experimental conditions that allow coincidence measurements. Total number of acquired traces: 10^7 . (a) Total ion (right) and total electron (top) time of flight spectra. Correlated events satisfying the condition of the existence of only one electron and one ion event in each trace (middle). (b) Electron energy spectrum including events correlated with single ionization (\circ), with double ionization (\bullet) and the distribution of the two ionic stages Xe^+ and Xe^{2+} .

rate resulting from the small acceptance solid angle of the set-up. Nevertheless the experiment clearly demonstrates that electron measurements correlated with Xe single and double ionization, as well as with background contributions are feasible with the new coincidence experimental procedure employed in the present work. Electrons originating from the background are recorded together with those originating from the ionization of Xe. The correlation of background ions with electrons is not shown here, because both the exact production process and the abundance of the background species are not known. Thus displaying these data has no physical meaning. The number of the false coincidence events can be estimated from the total electron events correlating with any produced ion, the electron events correlating with Xe^+ and those with Xe^{2+} . The error in the measured data due to the false coincidences is less than 4% in the present experiment. For the given detection efficiencies, false coincidences can be essentially neglected if the number of produced particle pairs is less than 1 per 30 laser shots [16]. The error bars shown in the following are thus one standard deviation of the number of events, which is practically the same as including the error due to the false coincidences.

In order to improve the statistics of the coincident events the results of few runs have been merged and the corresponding energy spectra are depicted in Figure 5.

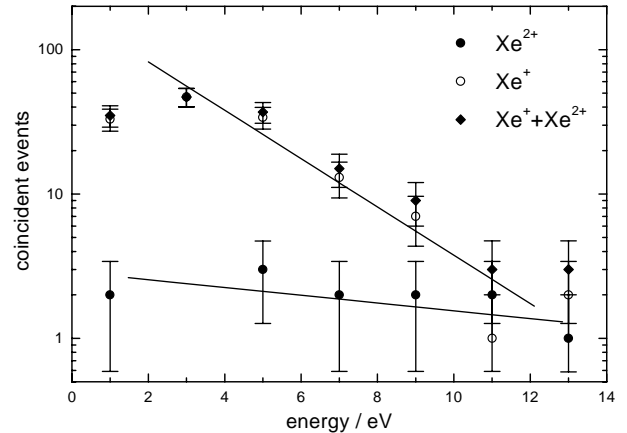


Fig. 5. Electron energy spectra correlated with single ionization (\circ), with double ionization (\bullet) and the sum of the two (\blacklozenge). Electrons correlated with double ionization contribute strongly to the high-energy part of the spectrum.

The runs have been performed under effectively the same experimental conditions. The total number of acquired traces amount to 2×10^7 . Electron events correlated with single ionization number 143, electrons correlated with double ionization are 13 and the sum of the two is 156. Due to the still low statistics no ATI peak, “plateau”, or any other detailed structure is observable in the spectra. The information that can be extracted from these spectra is the following:

- (i) the electron rate for the single ionization decreases at low energies;
- (ii) the electron rate drops with increasing energy much more rapidly for the single than for the double ionization up to an energy of 11 eV;
- (iii) the mean energy of the events is at 4.3 eV for the single ionization, and at 6.7 eV for the double ionization, that is the electron distribution that correlates with double ionization is “hotter”.

The general trend of the decreased rate at low energy in both coincidence and total spectra is most probably related with the drop of the spectrometer transmission, as well as with the broader angular distribution of the lower energy photoelectron ATI peaks [8] in combination with the small solid acceptance angle of the spectrometer. Nevertheless and at least as far as the transmission of the spectrometer is concerned, electron yields correlated with singly or doubly ionized species at a given energy can be compared. Such a comparison shows, within the limits of the low statistics of the experiment, that the events in the spectrum of electrons correlating with Xe^{2+} are much more prominent at higher energies and are practically negligible at the lower energy part of the spectrum. The contribution of electrons correlating with energies above 8 eV is of the order of 40%. Thus such electrons strongly contribute to the beginning of the “plateau” region of Figure 4b and seem, by extrapolation, to partially contribute to the “plateau” structure in general. However the statistics at present do not allow conclusive quantitative statement but only the outline of a qualitative trend.

4 Conclusions

In conclusion we have demonstrated feasibility of electron-ion coincidence measurements in short pulse high intensity interactions using a new experimental method. The method utilizes one and the same detection system for all particles and post-experiment software analysis of the data that allows the setting of multiple coincidence conditions (one electron and one singly ionized atom, one electron and one doubly ionized atom, two electrons and one doubly ionized atom etc.). The method and the same set up can be applied to any charged particles *e.g.* for ion-ion coincidence measurements for the study of photofragmentation processes of molecular species, or even electron-ion coincidence measurements in hybrid fragmentation-ionization experiments with molecules. The applicability limits of the method have been explored. A demonstration of the method has been presented in the ATI study of Xe in which a considerable contribution of double ionization in the higher energy part of the spectrum has been shown. The need for improved statistics in the experiment is apparent, in particular if quantitative conclusions are to be made or work at higher intensities and lighter elements is to be performed. Work towards this goal is currently in progress.

This work has been carried out in the Ultraviolet Laser Facility of FORTH with partial support from the TNR Program of the European Union (contract number ERBFMGECT950017). One of us (B.W.) Gratefully acknowledge support from the Alexander von Humboldt Stiftung No. 11461 (Lynen-Research Fellows of the AvH.) Enlightening discussions with D. Xenakis and C. Kalpouzos are gratefully acknowledged

References

1. A. L'Huillier, K.J. Schafer, K.C. Kulander, *J. Phys. B* **24**, 3315 (1991); A. L'Huillier, L.A. Lopré, G. Mainfray, C. Manus, in *Atoms in Intense Laser Fields*, edited by M. Gavrila (Academic Press, San Diego, 1992), pp. 132-206; E. Constant, D. Garzella, P. Breger, E. Mevel, C.H. Dorrer, C. Le Blanc, F. Salin, P. Agostini, *Phys. Rev. Lett.* **82**, 1668 (1999).
2. G. Varonov, N. Delone, *JETP Lett.* **1**, 66 (1965); P. Agostini, G. Barjot, J.F. Bonnal, G. Mainfray, C. Manus, *IEEE J. Quant. Electron.* **QE-4B**, 667 (1968); P. Lambropoulos, *Comm. At. Mol. Phys.* **20**, 199 (1987); M. Protopapas, C.H. Keitel, P.L. Knight, *Rep. Prog. Phys.* **60**, 389 (1997); A. Talebpour, C.-Y. Chien, S.L. Chin, *J. Phys. B* **29**, 5725 (1996).
3. L.J. Frasinski, K. Codling, P.A. Hatherly, *Science* **246**, 1029 (1989); D. Normand, C. Cornaggia, J. Lavancier, J. Morellec, in *Multiphoton Processes, Proc. of the 5th ICOMP*, edited by G. Mainfray, P. Agostini, Paris, 1990, p. 191; L. Frasinski, M. Stankiewicz, P.A. StHatherly, G.M. Cross, K. Codling, *Phys. Rev. A* **46**, R6789 (1992).
4. P. Agostini, F. Fabre, G. Mainfray, G. Petite, N.K. Raman, *Phys. Rev. Lett.* **42**, 1127 (1979); L.F. DiMauro, P. Agostini, *Adv. At. Mol. Opt. Phys.* **35**, 79 (1995).
5. A. L'Huillier, L.A. Lopré, G. Mainfray, C. Manus, *Phys. Rev. A* **27**, 2503 (1983); D. Charalambidis, P. Lambropoulos, H. Schröder, O. Faucher, *Phys. Rev. A* **50**, R2822 (1994); B. Walker, B. Sheehy, L.F. DiMauro, P. Agostini, K.J. Schafer, K.C. Kulander, *Phys. Rev. Lett.* **73**, 1227 (1994).
6. P. Lambropoulos, P. Maragakis, Jian Zhang, *Phys. Rep.* **305**, 203 (1998) and references therein.
7. G.G. Paulus, W. Nicklich, Xu Huale, P. Lambropoulos, H. Walther, *PRL* **72**, 2851 (1994).
8. G.G. Paulus, W. Nicklich, H. Walther, *Eur. Lett.* **27**, 267 (1994); V. Schyja, T. Lang, H. Helm, *Phys. Rev. A* **57**, 3692 (1997).
9. C.J.G.J. Uiterwaal, D. Xenakis, D. Charalambidis, *Z. Phys. D* **38**, 309 (1996); S.G. Preston, A. Sanpera, M. Zepf, W.J. Blyth, C.G. Smith, J.S. Wark, M.H. Key, K. Burnett, K. Nakai, M. Neely, A. Offenberger, *Phys. Rev. A* **53**, R31 (1996).
10. D. Normand, S. Dobosz, M. Lezius, P. D'Oliveira, M. Schmidt, in *Multiphoton Processes, Proc. of the 6th ICOMP*, edited by P. Lambropoulos, H. Walther, 1996, p. 287.
11. A. Zavriyev, P.H. Bucksbaum, *Phys. Rev. Lett.* **70**, 1077 (1993); C. Wunderlich, E. Kobler, H. Figger, T.W. Hänsch, *Phys. Rev. Lett.* **78**, 2333 (1997).
12. R. Wehlitz, F. Heisser, O. Hemmers, B. Langer, A. Menzel, U. Becker, *Phys. Rev. Lett.* **67**, 3764 (1991); P. Corkum, *Phys. Rev. Lett.* **71**, 1994 (1993); A. Becker, F.H.M. Faisal, *J. Phys. B* **29**, L197 (1996); T. Seidemann, M. Ivanov, P. Corkum, *PRL* **75**, 2819 (1995); S. Chelkowski, A. Bandrauk, *J. Phys. B* **28**, L723 (1995); M. Bewczyk, L. Frasinski, *J. Phys. B* **24**, L307 (1991).
13. B. Walker, E. Mevel, Baorui Yang, P. Breger, J.P. Chamaret, A. Antonetti, L.F. DiMauro, P. Agostini, *Phys. Rev. A* **48**, R894 (1993).
14. H. Rotke, C. Trump, M. Wittman, G. Korn, K. Hoffmann, W. Sandner (to appear in the *ICOMP VIII Proc.*); R. Doerner, Th. Weber, M. Weckenbroich, A. Staudte, L. Spielberger, O. Jagutzki, V. Mergel, F. Afaneh, G. Urbasch, H. Giessen, M. Vollmer (to appear in the *8th ICOMP VI Proc.*).
15. D. Strickland, G. Mourou, *Opt. Commun.* **56**, 219 (1985).
16. V. Stert, W. Radloff, C.P. Schulz, I.V. Hertel, *Eur. Phys. J. D* **5**, 97 (1999).
17. B. Brehm, J. Grosser, T. Ruscheinski, M. Zimmer, *Meas. Sci. Technol.* **6**, 953 (1995).